Yaw-misalignment and its impact on wind turbine loads and wind farm power output

van Dijk, M.T.; van Wingerden, Jan-Willem; Ashuri, T.; Li, Y.; Rotea, M.A.

DOI
10.1088/1742-6596/753/6/062013

Publication date
2016

Document Version
Final published version

Published in
Journal of Physics: Conference Series

Yaw-Misalignment and its Impact on Wind Turbine Loads and Wind Farm Power Output

Mike T. van Dijk and Jan-Willem van Wingerden
Delft Center for Systems and Control, Delft University of Technology, Delft, 2628 CD, the Netherlands

Turaj Ashuri
Department of Mechanical Engineering, Arkansas Tech University, 1811 N Boulder Ave, Russellville, AR 72801, USA

Yaoyu Li and Mario A. Rotea
Department of Mechanical Engineering, University of Texas at Dallas, Richardson, TX 75080, USA

Abstract. To make wind energy cost competitive with traditional resources, wind turbines are commonly placed in groups. Aerodynamic interaction between the turbines causes sub-optimal energy production. A control strategy to mitigate these losses is by redirecting the wake by yaw misalignment. This paper aims to assess the influence of load variations of the rotor due to partial wake overlap and presents a combined optimization of the power and loads using wake redirection. For this purpose, we design a computational framework which computes the wind farm power production and the wind turbine rotor loads based on the yaw settings. The simulation results show that partial wake overlap can significantly increase asymmetric loading of the rotor disk and that yaw misalignment is beneficial in situations where the wake can be sufficiently directed away from the downstream turbine.

1. Introduction

In recent years, wind energy has evolved as a reliable source among all the renewable energy resources [1–5]. However, the cost of wind generated electricity is generally higher than that of traditional energy resources [6]. This necessitates further research and innovation of the design and operation of wind turbines that can reduce cost of energy [7–15].

An effective strategy to cost reduction is to group wind turbines to share the infrastructure. As a consequence when an upwind wind turbine extracts energy from the wind, a speed deficit and increased turbulence occur in it's wake. Therefore, downstream wind turbines produce less power, and they experience altered loads. Hence, the control parameters of upstream turbines are coupled with the power production and loads of downstream turbines. The significance of such coupling manifests for smaller turbine spacing, as the wake has less time to recover. Because traditional control strategies maximize the individual wind turbine, this phenomenon is not addressed from the perspective of the total power of a wind farm. Accordingly, optimal power production of the wind farm is not guaranteed.

This problem can be mitigated using control strategies that take into account the wake effects. One approach is to decrease the power extraction of upstream turbines to improve the

performance of downstream turbines, thus increasing the total wind farm power production. This method has been investigated in multiple simulation studies. Marden et al. [16] increased the power of an array of wind turbines by 25% using a game-theoretic approach. Gebraad and Wingerden [17] maxized the power production with the application of a model-free gradient-based algorithm. Yang et al. [18] applied an Extremum seeking control algorithm in a nested-loop framework, that optimized the array from downstream to upstream units in a sequential manner. Rotea [19] has shown that wind farm optimization problems may be solved with dynamic programming, which reduces the complexity of the optimization and provides a formal mechanism for computing limits of performance in wind farms, as well as rigorous proof that the nested loop extremum seeking control approach advanced in Santoni et al. [20] is optimal. Goit and Meyers [21] used a high fidelity simulation in combination with a conjugate gradient optimization algorithm. Corten and Schaak [22] performed a wind tunnel experiment of three rows of 8 scaled turbines and concluded that the power extraction could be increased by derating the upstream turbines.

Another, more recent approach is by introducing yaw-misalignment in the upwind turbines to redirect the wake away from downstream turbines. Several simulation studies have shown the benefits of yaw misalignment. Gebraad et al. [23] increased the power output of a simulated wind farm by yaw misalignment using a game-theoretic optimization approach, and a data-driven parametric model for wake effects [24]. Park and Law [25] performed a wind tunnel test of two turbines by applying a Bayesian optimization algorithm, using yaw and blade pitch as inputs. Fleming et al. [26] performed a combined optimization of yaw control and lay-out to improve the cost of energy of wind farms. Churchfield et al. [27] found an increased power output for an array of turbines when yaw-misalignment in the neighborhood of 20% was imposed on the upstream turbines, using a large-eddy simulation.

Despite these benefits of enhancing energy capture, yaw misalignment has potential to influence the loads of each turbine. Kragh and Hansen [28] suggested that the blade out-of-plane bending moments of upstream turbines decrease by a yaw-misalignment in the range of -10 to 30 degrees, depending on the wind speed. Fleming et al. [29] found similar results using SOWFA [30, 31] for a two turbine case. They also found that the downstream turbine showed an increased out-of-plane bending moment, drivetrain torsion and tower-base bending moment. These loads are likely caused by the transition from full to partial wake overlap. Boorsma [32], Ashuri and Zaaijer [33] and Capponi et al. [34] revealed that the blade edgewise moments are mainly dominated by gravity force. On the other hand, the blade out-of-plane loads vary with yaw-misalignment. Churchfield et al. [27] showed an increase in the blade out-of-plane bending moments of downstream turbines due to yaw misalignment.

As the literature shows, yaw misalignment can increase the power output, but also has a significant effect on the loads of wind turbines. To decrease the cost of wind energy, it is important to increase the power production without significantly reducing the lifetime of a wind turbine. Therefore, any application of control algorithms should not have a negative impact on the loads. This research assesses the load variations due to partial wake overlap as well as yaw misalignment. Also, the optimal yaw misalignment settings are found that maximize the power production of a wind farm while taking into account load variations of the flap and edgewise moments.

2. Computational Framework

We developed a computational framework to analyze the impact of wake effects on the power production and loading. A wind farm consisting of NREL 5MW baseline turbines [35] is used. The loads considered are the maximum-to-minimum difference of the flap and edgewise moments (Section 2.3). These are chosen to capture the asymmetric load distribution on a rotor blade due to partial wake overlap. To facilitate this, an algorithm that computes the velocity distribution

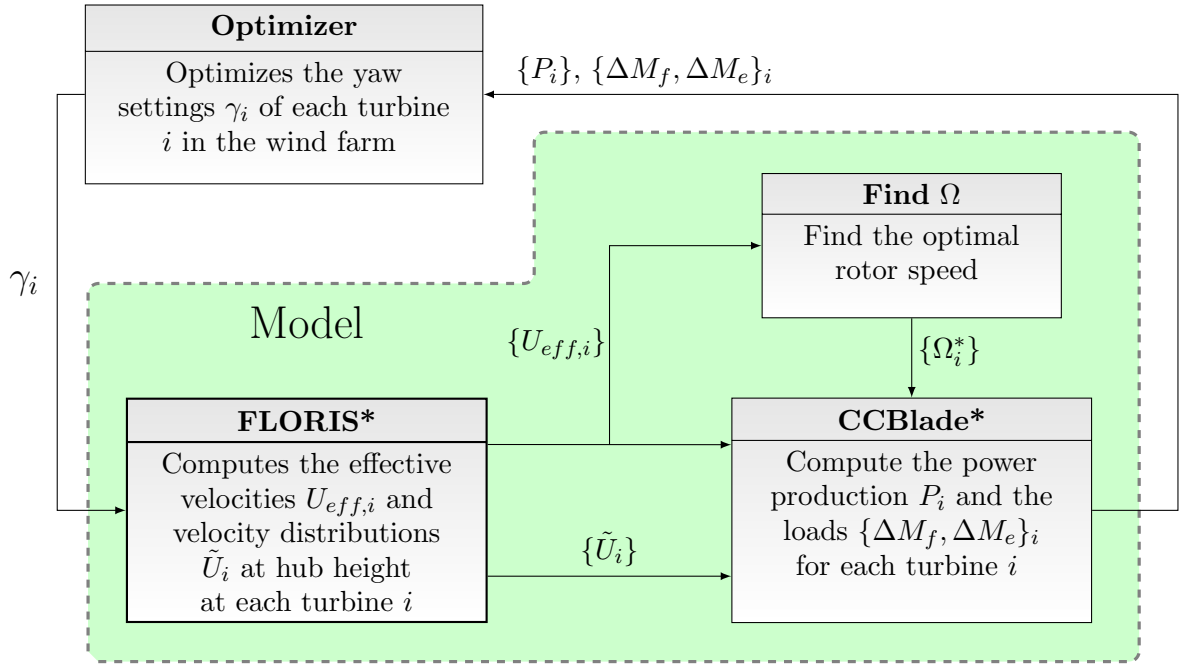

Figure 1: Schematic of the optimization framework. The optimizer uses the power and load measurements obtained from the model to optimize the yaw settings of the wind farm. The shorthand notation $\{\zeta_i\}$ is used to indicate that $\{\zeta_i | i \in \mathcal{U}\}$ where ζ_i corresponds to a property of wind turbine i and $\mathcal{U} = \{1, 2, ..., N\}$ is the set of indices that number all turbines in a wind farm.

at the rotor disk is implemented as described in Section 2.1.

Figure 1 shows the framework that consists of a modified version of the FLOw Redirection and Induction in Steady-state (FLORIS) model [24], a modified version of CCBlade [36] and an optimizer [1,2]. In the *FLORIS** module, the effective wind velocities and velocity distributions in the lateral direction at hub height at each wind turbine are calculated. The module '*Find* Ω' determines the optimal rotor velocity for every turbine based on the effective wind velocity. The optimal rotor velocity and the velocity distribution are used to compute the power production and the loads at every turbine in the module *CCBlade**. The *Optimizer* subsection closes the loop by including the power production and the loads of the wind farm in one cost function, and is used to find the optimal yaw settings.

*2.1. FLORIS**

FLORIS* is an extended version of FLORIS, in that it adds an algorithm that computes the velocity distribution at hub height. FLORIS is a data-driven model that predicts the effect of yaw-misalignment on the power production of wind turbines in a wind farm. FLORIS models the wake using a modified version of the Jensen model [37] and characterizes the wake deflection as in [38]. The fidelity of the model is increased by dividing the wake in three zones with individual expansion and velocity properties (Figure 2). Furthermore, the model is augmented to fit with power measurements obtained through high-fidelity simulations.

FLORIS defines a local system of coordinates (x, y) relative to the global system of coordinates (x', y') based on the wind direction Φ. The wake deflection of a turbine i is calculated using its

[1] FLORIS: https://github.com/WISDEM/FLORISSE, accessed: 04-March-2016
[2] CCBlade: https://github.com/WISDEM/CCBlade, accessed: 04-March-2016

yaw γ_i. For a wake caused by turbine j, the velocity in each corresponding wakezone z at the x-coordinate of a turbine i is defined by $U_{j,i,z}$, $z \in \{1, 2, 3\}$. FLORIS computes the effective wind velocity, $U_{eff,i}$, at a downstream turbine i by combining all the overlapping wakes at its rotor disk. This is done by weighting the wake velocities $U_{j,i,z}$ by their overlap of the corresponding wake zones with the rotor disks using the root-sum-square method of [39].

FLORIS* extends this model with an algorithm that computes the velocity distribution at hub height. We introduce the set of indices $\mathcal{U} = \{1, 2, ..., N\}$ that number all turbines in a wind farm. Each turbine $j \in \mathcal{U}|_{j \neq i}$ has a velocity distribution over turbine i denoted by $\tilde{U}_{j,i}(y_{r,i})$ provided by FLORIS. The local y-coordinate on the rotor disk of turbine i at hub height is denoted by $y_{r,i}$ as shown in Figure 3. We define the combined velocity distribution $\tilde{U}_i(y_{r,i})$ over the rotor blade of turbine i with radius R. Now for any $y_{r,i}$ in the range $[-R, R]$, we obtain $\tilde{U}_i(y_{r,i})$ by applying the root-sum-square method:

$$\tilde{U}_i(y_{r,i}) = U_\infty \left(1 - \sqrt{\sum_{j \in \mathcal{U} \setminus \{i\}} \left(1 - \frac{\tilde{U}_{j,i}(y_{r,i})}{U_\infty} \right)^2} \right) \tag{1}$$

where U_∞ is the velocity of the incoming wind flow.

2.2. Computation of the optimal rotor velocities

Each turbine has a steady-state rotational speed based on the effective wind velocity it experiences which needs to be determined. At below rated wind speeds every turbines internal controller will try to maximize its power production [40, 41]. This corresponds to maximizing the power coefficient $Cp(\lambda_{tip}, \beta)$, which can be modeled as a function of tip-speed-ratio λ_{tip} and blade pitch β [42, 43]. We estimate the optimal steady-state rotor speed Ω_i^* for turbine i by:

$$\Omega_i^* = \frac{\lambda_{tip,i}^* * U_{eff,i}}{R} \tag{2}$$

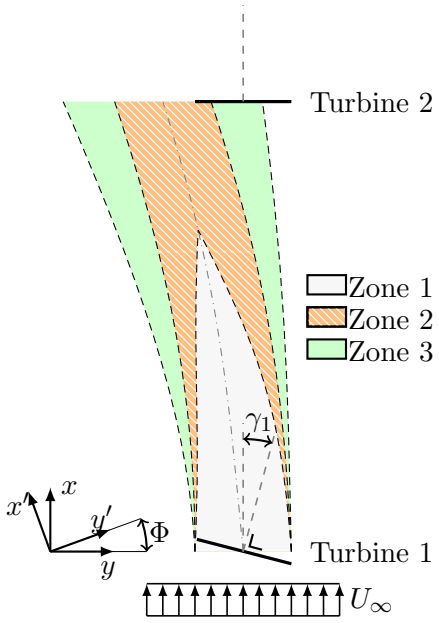

Figure 2: A schematic overview of a wake deflected by yaw misalignment, as modeled by FLORIS. The different wake zones are indicated.

where λ_i^* is the tip-speed-ratio that maximizes the corresponding power coefficient $Cp_i(\lambda_i^*, \beta_i)$, β_i is assumed to be 0 which is optimal for below rated wind speeds and $U_{eff,i}$ is the local effective wind velocity. The Cp-table is obtained using *Wt perf* [44] which is a simulation tool developed by NREL that uses blade-element momentum theory to predict the performance of wind turbine blades.

*2.3. CCBlade**

CCBlade* is an extended version of CCBlade, in that it adds an algorithm to compute the load variations due to partial wake overlap. CCBlade is an implementation of a reliable method to solve the blade element momentum (BEM) equations [45] and predicts the aerodynamic power production and loading of wind turbine blades. For each turbine i in the wind farm, the model uses the effective wake velocity $U_{eff,i}$ and the optimal steady-state rotor speed Ω_i^* for its computations. These will be used to compute the power (P_i) of each turbine. The model is extended by taking into account the velocity distribution at hub height $\tilde{U}_i(y_{r,i})$ in order to compute the maximum-to-minimum difference of the flapwise ($\Delta M_{f,i}$) and edgewise ($\Delta M_{e,i}$) bending moments. As the rotor blade will experience these extreme loads during one rotation, these terms will be used analogously to fatigue.

CCBlade will determine how much each section of the blade at each azimuth angle contributes to the total thrust and torque of a wind turbine. These contributions are denoted respectively as $Q_p(r, \Phi)$ and $T_p(r, \Phi)$ where r is the radial coordinate of the rotor disk. Now the total thrust force F_T and torque Q over one rotor rotation can be determined by:

$$F_T(r,\Phi) = N_b \int_0^{2\pi} \int_0^R Q_p(r,\Phi)\, dr\, d\Phi, \qquad Q_p(r,\Phi) = N_b \int_0^{2\pi} \int_0^R T_p(r,\Phi)\, dr\, d\Phi \tag{3}$$

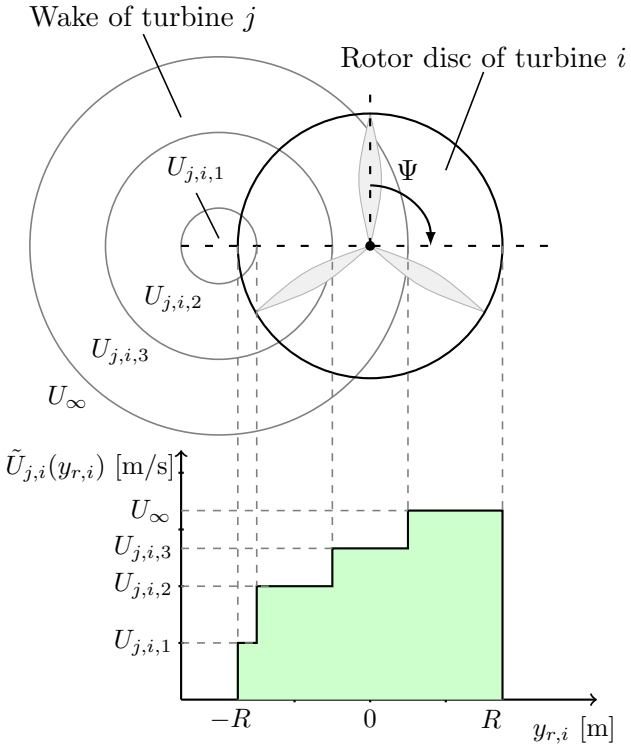

Figure 3: Velocity distribution $\tilde{U}_{j,i}(r)$ at hub height of a wind turbine i with radius R, partially overlapped by the wake of turbine j

where N_b represents the number of blades ($N_b = 3$). The aerodynamic power, assuming an optimal rotor speed, can be computed by:

$$P = Q_p(r, \Phi) * \Omega_i^* \tag{4}$$

Finally, the maximum-to-minimum difference of the flap and edgewise moments are determined. To be able to detect the influence of partial wake overlap on the loading, CCBlade* is expanded to take into account a velocity distribution instead of the uniform effective velocity distribution U_{eff}. Because the greatest difference in loading due to partial wake overlap is expected to happen between the loads at $\Phi = 90°$ and $\Phi = 270°$, we use the velocity distribution $\tilde{U}_i(y_{r,i})$ at hub height. The maximum-to-minimum flapwise and edgewise bending moment differences are computed as follows:

$$\Delta Mf = |Mf_{\Phi=90°} - Mf_{\Phi=270°}|, \quad \Delta Me = |Me_{\Phi=90°} - Me_{\Phi=270°}| \tag{5}$$

2.4. Optimizer

The optimizer utilizes a Game-theoretic (GT) optimization approach [16] to find the set of yaw-settings $\boldsymbol{\gamma} = \{\gamma_1, \gamma_2, ..., \gamma_N\}$ that maximizes the power production and minimizes the loads of the wind farm. To achieve the objective, a constrained minimization problem is defined as follows:

$$\begin{aligned} &\underset{\boldsymbol{\gamma}}{\text{minimize}} \quad c(\boldsymbol{\gamma}) \\ &\text{subject to} \quad |\gamma_i| \leq \gamma_{max},\ i = 1, \ldots, N \end{aligned} \tag{6}$$

where γ_{max} is the maximum allowable yaw angle and is chosen to be $\gamma_{max} = 40°$. This constraint is added to limit the search space. The cost functional $c(\boldsymbol{\gamma})$ combines the power and the loads of a turbine $i \in \mathcal{U}$ as follows:

$$\begin{aligned} c(\boldsymbol{\gamma}) &= -\lambda \underbrace{\left(\sum_{i=1}^{N}\right) \overline{P}_i(\boldsymbol{\gamma})}_{power} + \frac{(1-\lambda)}{2N} \underbrace{\left(\sum_{i=1}^{N} \Delta\overline{M}_{f,i}(\boldsymbol{\gamma}) + \sum_{i=1}^{N} \Delta\overline{M}_{e,i}(\boldsymbol{\gamma})\right)}_{loads} \\ \overline{P}_i(\boldsymbol{\gamma}) &= \frac{P_i(\boldsymbol{\gamma})}{\widetilde{P}_{max}}, \qquad \Delta\overline{M}_{f,i}(\boldsymbol{\gamma}) = \frac{\Delta M_{f,i}(\boldsymbol{\gamma})}{\Delta\widetilde{M}_{f,max}}, \qquad \Delta\overline{M}_{e,i}(\boldsymbol{\gamma}) = \frac{\Delta M_{e,i}(\boldsymbol{\gamma})}{\Delta\widetilde{M}_{e,max}} \end{aligned} \tag{7}$$

where $\overline{P}_i$, $\Delta\overline{M}_{f,i}$ and $\Delta\overline{M}_{e,i}$ are respectively the normalized power and the maximum variation in the flapwise and edgewise bending moments of turbine i. The tuning parameter of the optimization objective is λ, where $\lambda = 1$ corresponds to a single-objective optimization of the power production and $\lambda = 0$ of the loads. Any intermediary values would define a multi-objective optimization. Finally, $\widetilde{P}_{max}$, $\Delta\widetilde{M}_{f,max}$ and $\Delta\widetilde{M}_{e,max}$ are respectively the estimations of the maximum possible values of the power, flapwise bending moment and edgewise bending moment of a turbine at a certain wind speed which are obtained through a series of simulations (see Section 3.1).

The GT approach makes random perturbations to the yaw settings and sets these as the new baseline if they yield an improvement over the previous baseline (see [24]). Using this approach, the global minimum is iteratively found. The decision for this algorithm was based on the discovery of many local minima in the objective function which are caused by the discrete nature of the velocities in the different wake zones.

3. Results

In this section, the results of two simulation scenarios are presented. In the first scenario, a downstream turbine is swept through the wake of an upstream turbine in order to study the effects of partial wake overlap on the power and the loads. The second scenario will consist of various cases in which the yaw settings of an array of two turbines are optimized using a GT-approach. All simulations are done assuming a constant wind velocity of $U_\infty = 8$ m/s.

3.1. The effect of partial wake overlap on power production and loads

The first simulation setup consists of an array of two wind turbines (Figure 4), spaced 6 rotor diameters apart in the x direction while both turbines are yawed into the wind. The effects of partial wake overlap are investigated by sweeping turbine 2 through the wake of turbine 1 in the y-direction. The distance from the center of turbine 1 to the y-coordinate of turbine 2 is indicated by dY. The results of this simulation are used to obtain the maximum values $\widetilde{P}_{max}$, $\widetilde{M}_{f,max}$ and $\widetilde{M}_{e,max}$ in the cost functional (Equation 7).

The results are shown in Figure 5. It can be seen that partial wake overlap results in a significant increase in the loads, which is unfavorable. Furthermore, the loading and power production are not completely symmetric over the range of dY. The maximum loading is higher when the center of turbine 2 is above the wake center. This is likely caused by the effect of the rotational direction of the rotor blade on the wake. Furthermore, several degrees of wake overlap differently affect the power production and the loads. Full symmetric wake overlap (dY=0 m) results in close-to-minimum loading but also sub-optimal power production. Partial wake overlap (i.e. dY=80 m) comes with an increased power production, but also significantly increases the loads. Finally, no wake overlap (i.e. dY=170 m) maximizes both the power and minimizes the loads. In the situation where dY=0, these optima might not be feasible by just yawing turbine 1 as the maximum amount of wake deflection through yawing is limited. This forms motivation for the claim that the potential load reduction while increasing the power production for a given wind farm layout will strongly depend on the wind direction.

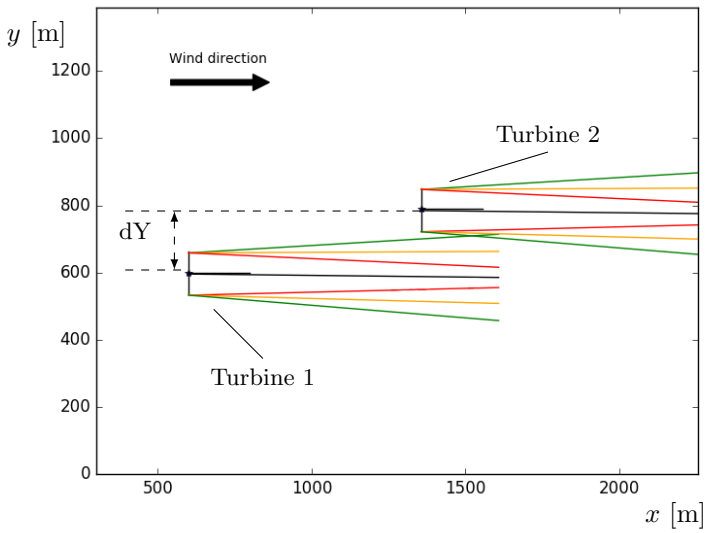

Figure 4: Lay-out consisting of 2 turbines with an incoming wind velocity of $U_\infty = 8$ m/s. Turbine 2 is swept through the wake of turbine 1

3.2. Optimization of the power and the loads

In this section, the optimization results are presented for an array of two turbines which corresponds to Figure 4 for dY=0. The optimization is performed using a mixed-objective cost-function (Equation 7) for various Φ at a windspeed of 8 m/s. The optimization was run for 4000 iterations with an exploration factor $E_e = 0.4$. For each windspeed, the following cases will be considered:

- Baseline: The yaw-settings are chosen such that both turbines maximize their individual power production. These settings are referred to as *greedy*.
- Case 1 (λ=1): Single-objective optimization of the power.
- Case 2 (λ=0.97): Multi-objective optimization of both the power and the loads.
- Case 3 (λ=0.90): Similar to Case 2, with a stronger emphasis on the loads.
- Case 4 (λ=0): Single-objective optimization of the loads.

The results are presented in Table 1. The optimized yaw settings are shown in Table 2. A trend can be seen in each case over all wind directions. An optimization of the power ($\lambda = 1$) will steer the wake of turbine 1 away from the downstream turbine, striving for zero wake overlap. The minimization of the loads ($\lambda = 0$) will set the yaw of turbine 1 so that the wake is evenly

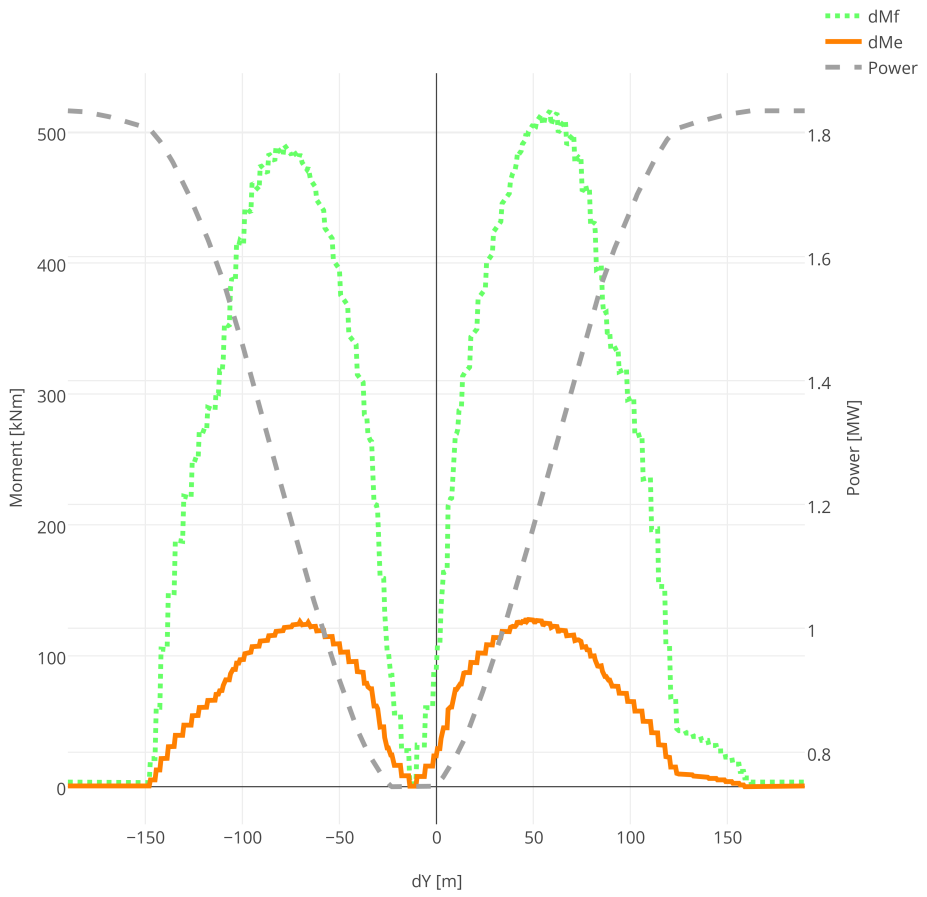

Figure 5: The normalized power production, maximum-to-minimum flapwise moment and edgewise moment of turbine 2 versus dY

Table 1: Optimization results for various cost functions and wind directions of a 2-turbine array. The results are expressed in % change compared to the baseline case

		P_{tot}	$\sum \Delta M_f$	$\sum \Delta M_e$
0°	$\lambda = 1$	3.75	342.71	352.89
	$\lambda = 0.97$	3.58	304.53	313.06
	$\lambda = 0.90$	-1.02	-93.99	-96.17
	$\lambda = 0$	-18.69	-95.35	-96.76
5°	$\lambda = 1$	5.49	-5.14	163.90
	$\lambda = 0.97$	5.39	-10.07	150.97
	$\lambda = 0.90$	5.39	-10.07	150.97
	$\lambda = 0$	-53.01	-93.21	-84.20
10°	$\lambda = 1$	0.98	-66.35	-93.01
	$\lambda = 0.97$	0.92	-86.98	-96.95
	$\lambda = 0.90$	0.68	-95.59	-99.38
	$\lambda = 0$	-57.85	-98.45	-99.67

distributed over the rotor disk of the downstream turbine, or if possible, is avoided all together. The combined optimizations ($\lambda = 0.97$ and $\lambda = 0.90$) find a trade-off between the two objectives.

In general, optimizing the power production through yaw-misalignment heavily increases the loads for $\Phi = 0$, and decreases the loads for $\Phi = 5°$ and $\Phi = 10°$. In the case of $\Phi = 0°$, there is only a small reduction in loads possible without heavily penalizing the power production. For $\Phi = 5°$ and $\Phi = 10°$, Case 1-3 will result in both an increase in power, and a great reduction in loading compared to the baseline. This has to do with the fact that partial wake overlap was already present before the optimization. Case 2 and 3 are able to achieve additional reductions in loading opposed to Case 1 at the expense of a small amount of power production.

The Pareto fronts of the cumulative power and differential loading for various wind directions are depicted in Figure 6. It can be seen that for $Phi = 0°$, increasing the power comes with an inevitable increase of differential loading. For $\Phi = 5°$ and $\Phi = 10°$, more of a trade-off can be made between power and loading. The use of a mixed-objective optimization is most beneficial for $\Phi = 10°$, as a significant loading decrease can be obtained at the expense of a small amount of power production.

Table 2: Resulting yaw settings of the various optimizations

	Baseline		Case 1 ($\lambda = 1$)		Case 2 ($\lambda = 0.97$)		Case 3 ($\lambda = 0.90$)		Case 4 ($\lambda = 0$)	
	γ_1	γ_2	γ_1	γ_2	γ_1	γ_2	γ_1	γ_2	γ_1	γ_2
$\Phi = 0°$	0°	0°	15.5°	0.3°	15.2°	0.3°	−4.9°	0.3°	−6.8°	−40°
$\Phi = 5°$	0°	0°	−13.6°	0.4°	−15.2°	0.3°	−15.2°	0.3°	39.9°	−39.9°
$\Phi = 10°$	0°	0°	−5.2°	0.3°	−6.5°	0.4°	−7.9°	0.3°	−40°	−40°

4. Conclusion and Discussion

This paper studies the load variations due to partial wake overlap and the optimal yaw misalignment to maximize the power production while taking into account the loads variations. The power production and loads were computed using an optimization framework that modeled yaw misalignment, wake interaction and partial wake overlap for multi-turbine setups. In the first simulation, the effect of partial wake overlap on the power production and the loads was investigated (Section 3.1). It was found that partial wake-overlap greatly increases the maximum-to-minimum flapwise and edgewise bending moments compared to full symmetrical wake overlap. The preliminary results suggest that yaw misalignment of upstream turbines

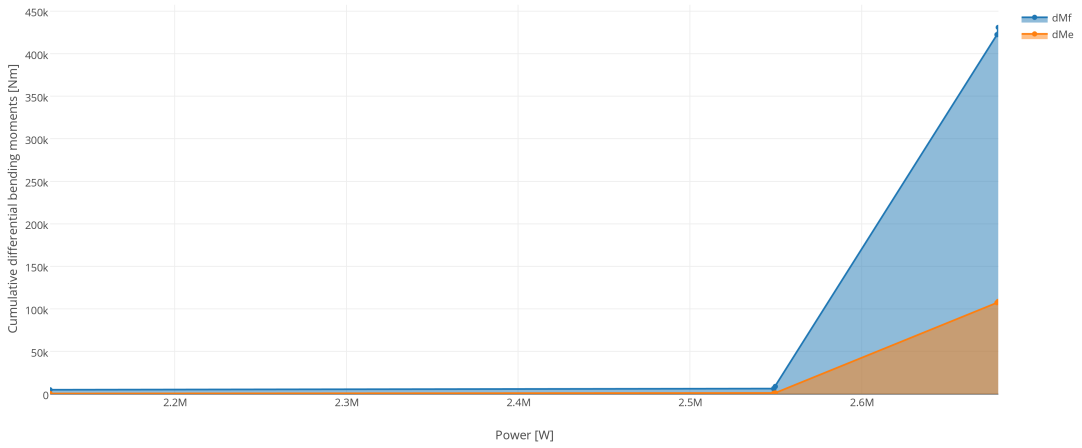

(a) Wind direction of 0°

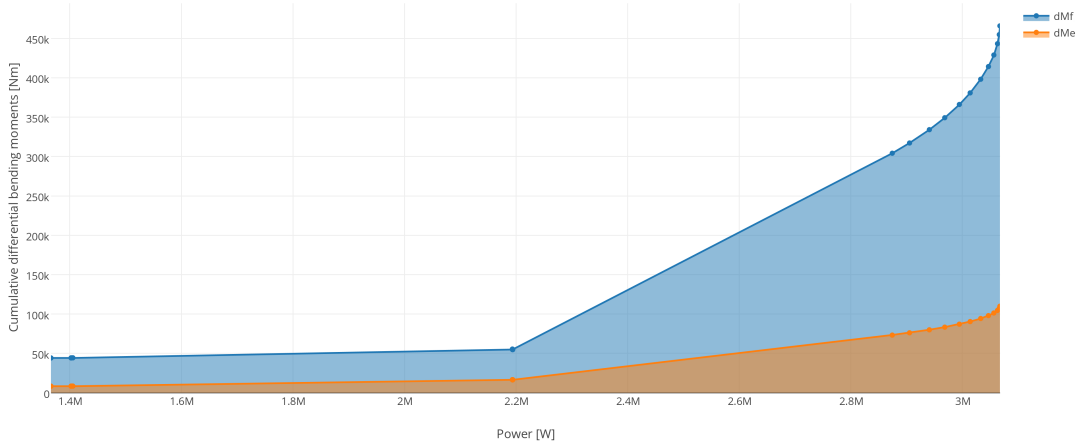

(b) Wind direction of 5°

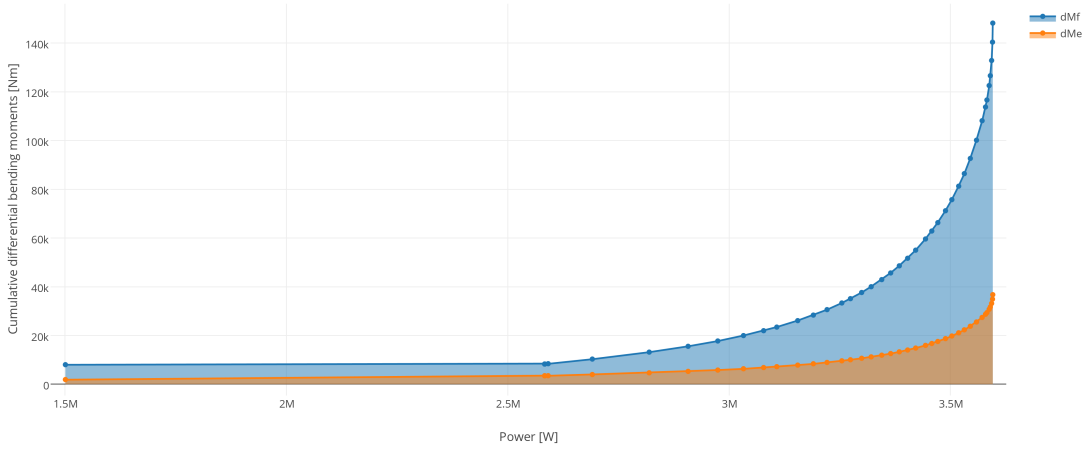

(c) Wind direction of 10°

Figure 6: Pareto fronts of total power and cumulative differential loading for various wind directions

is a desirable solution in situations where the wake can be sufficiently redirected away from downstream turbines.

This idea was confirmed in the second simulation, where an array of two turbines was optimized using a GT optimization approach for various cases (Section 3.2). It was shown that optimizing for power will result in a significant increase up to 350% in loading for $\Phi = 0°$ but in a decrease for $\Phi = 5°$ and $\Phi = 10°$. This suggests that yaw misalignment isn't equally beneficial for all wind directions, and that its benefits depend on the topology and wind direction of a wind farm. Finally, a combined optimization of power and loads is shown to be beneficial as in the previously mentioned situations, a decrease in loading can be realized at a small expense of the power production.

This work presents preliminary results of mixed-objective wind farm optimization using yaw misalignment and is bound to a number of limitations. Our optimization framework uses a steady-state model for computational efficiency, and therefore transitional effects and turbulence are not taken into account. Furthermore, although FLORIS has been validated using SOWFA simulation data, the load computations have not. Finally, the GT optimization approach is not guaranteed to converge on a global optimum as the number of iterations executed is smaller than the total search space due to time constraints.

In future work, a simulation of the proposed combined optimization of power and loads is to be extended to a full-scale wind farm for a complete range of possible wind directions. Furthermore, a dynamic model may be used for simulation purposes as this will allow us to investigate important loading phenomena such as the transition of partial to full wake overlap and the application of more sophisticated algorithms to compute fatigue loading. Finally, the results ought to be validated using high-fidelity simulations, for instance by using SOFWA coupled with FAST [46].

References

[1] Eleanor Denny. The economics of tidal energy. *Energy Policy*, 37(5):1914–1924, 2009.

[2] Nathan S Lewis. Toward cost-effective solar energy use. *science*, 315(5813):798–801, 2007.

[3] Ralph EH Sims, Hans-Holger Rogner, and Ken Gregory. Carbon emission and mitigation cost comparisons between fossil fuel, nuclear and renewable energy resources for electricity generation. *Energy policy*, 31(13): 1315–1326, 2003.

[4] Patrick Sullivan, Wesley Cole, Nate Blair, Eric Lantz, Venkat Krishnan, Trieu Mai, David Mulcahy, and Gian Porro. 2015 standard scenarios annual report: Us electric sector scenario exploration. Technical report, National Renewable Energy Laboratory (NREL), Golden, CO (United States), 2015.

[5] Turaj Ashuri, Gerard Bussel, and Stefan Mieras. Development and validation of a computational model for design analysis of a novel marine turbine. *Wind Energy*, 16(1):77–90, 2013.

[6] Mark Bolinger and Ryan Wiser. Wind power price trends in the united states: struggling to remain competitive in the face of strong growth. *Energy Policy*, 37(3):1061–1071, 2009.

[7] Turaj Ashuri, Tao Zhang, Dong Qian, and Mario Rotea. Uncertainty quantification of the levelized cost of energy for the 20MW research wind turbine model. In *AIAA Science and Technology Forum and Exposition (SciTech), Wind Energy Symposium, San Diego, California*, page 1998. AIAA, 2016.

[8] María Isabel Blanco. The economics of wind energy. *Renewable and Sustainable Energy Reviews*, 13(6): 1372–1382, 2009.

[9] Turaj Ashuri, Mario Rotea, Yan Xiao, Yaoyu Li, and Chandra Verma Ponnurangam. Wind turbine performance decline and its mitigation via extremum seeking controls. In *AIAA Science and Technology Forum and Exposition (SciTech), Wind Energy Symposium, San Diego, California*, pages 1–11. AIAA, 2016.

[10] F Spinato, Peter J Tavner, GJW Van Bussel, and E Koutoulakos. Reliability of wind turbine subassemblies. *Renewable Power Generation, IET*, 3(4):387–401, 2009.

[11] Turaj Ashuri, Michiel B Zaaijer, Joaquim RRA Martins, Gerard JW van Bussel, and Gijs AM van Kuik. Multidisciplinary design optimization of offshore wind turbines for minimum levelized cost of energy. *Renewable Energy*, 68(0):893–905, 2014.

[12] E Echavarria, B Hahn, GJ van Bussel, and T Tomiyama. Reliability of wind turbine technology through time. *Journal of Solar Energy Engineering*, 130(3):031005, 2008.

[13] Turaj Ashuri and Michiel B Zaaijer. Review of design concepts, methods and considerations of offshore wind turbines. In *European Offshore Wind Conference and Exhibition, Berlin, Germany*, pages 1–10. European Wind Energy Association, 2007.

[14] Peter Jamieson. *Innovation in wind turbine design*. John Wiley & Sons, 2011.

[15] JW Van Wingerden, AW Hulskamp, T Barlas, B Marrant, GAM Van Kuik, DP Molenaar, and M Verhaegen. On the proof of concept of a'smart'wind turbine rotor blade for load alleviation. *Wind Energy*, 11(3):265, 2008.

[16] Jason R Marden, Shalom D Ruben, and Lucy Y Pao. A model-free approach to wind farm control using game theoretic methods. *Control Systems Technology, IEEE Transactions on*, 21(4):1207–1214, 2013.

[17] PMO Gebraad and JW Wingerden. Maximum power-point tracking control for wind farms. *Wind Energy*, 18(3):429–447, 2015.

[18] Zhongzhou Yang, Yaoyu Li, and John E Seem. Optimizing energy capture of cascaded wind turbine array with nested-loop extremum seeking control. *Journal of Dynamic Systems, Measurement, and Control*, 137 (12):121010, 2015.

[19] Mario A Rotea. Dynamic programming framework for wind power maximization. In *Proc. of the 19th IFAC World Congress, Cape Town, South Africa*, pages 3639–3644, 2014.

[20] Christian Santoni, Umberto Ciri, Mario Rotea, and Stefano Leonardi. Development of a high fidelity cfd code for wind farm control. In *American Control Conference (ACC), 2015*, pages 1715–1720. IEEE, 2015.

[21] Jay P Goit and Johan Meyers. Optimal control of energy extraction in wind-farm boundary layers. *Journal of Fluid Mechanics*, 768:5–50, 2015.

[22] GP Corten and P Schaak. Heat and flux: Increase of wind farm production by reduction of the axial induction. In *Proceedings of the European Wind Energy Conference*, 2003.

[23] PMO Gebraad, FW Teeuwisse, JW Wingerden, PA Fleming, SD Ruben, JR Marden, and LY Pao. Wind plant power optimization through yaw control using a parametric model for wake effects—a cfd simulation study. *Wind Energy*, 19(1):95–114, 2016.

[24] Pieter MO Gebraad, FW Teeuwisse, Jan-Willem van Wingerden, Paul A Fleming, Shalom D Ruben, Jason R Marden, and Lucy Y Pao. A data-driven model for wind plant power optimization by yaw control. In *American Control Conference (ACC), 2014*, pages 3128–3134. IEEE, 2014.

[25] Jinkyoo Park and Kincho H Law. A bayesian optimization approach for wind farm power maximization. In *SPIE Smart Structures and Materials+ Nondestructive Evaluation and Health Monitoring*, pages 943608–943608. International Society for Optics and Photonics, 2015.

[26] Paul A Fleming, Andrew Ning, Pieter MO Gebraad, and Katherine Dykes. Wind plant system engineering through optimization of layout and yaw control. *Wind Energy*, 19(2):329–344, 2016.

[27] M Churchfield, P Fleming, B Bulder, and S White. Wind turbine wake-redirection control at the fishermen's atlantic city windfarm: Preprint. Technical report, NREL (National Renewable Energy Laboratory (NREL), Golden, CO (United States)), 2015.

[28] Knud A Kragh and Morten H Hansen. Load alleviation of wind turbines by yaw misalignment. *Wind Energy*, 17(7):971–982, 2014.

[29] Paul Fleming, Pieter MO Gebraad, Sang Lee, Jan-Willem Wingerden, Kathryn Johnson, Matt Churchfield, John Michalakes, Philippe Spalart, and Patrick Moriarty. Simulation comparison of wake mitigation control strategies for a two-turbine case. *Wind Energy*, 18(12):2135–2143, 2015.

[30] Nwtc information portal (sowfa). `https://nwtc.nrel.gov/SOWFA`.

[31] Matthew J Churchfield, Sang Lee, John Michalakes, and Patrick J Moriarty. A numerical study of the effects of atmospheric and wake turbulence on wind turbine dynamics. *Journal of turbulence*, (13):N14, 2012.

[32] K Boorsma. Power and loads for wind turbines in yawed conditions. Technical report, ECN-E-12-047, ECN, Petten, The Netherlands, 2012.

[33] Turaj Ashuri and MB Zaaijer. Size effect on wind turbine blade's design drivers. In *Europeain Wind Energy Conference and exhibition, Brussels, Belgium*, pages 1–6. European Wind Energy Association, 2008.

[34] Pablo Castillo Capponi, Turaj Ashuri, Gerard JW van Bussel, and Bjarne Kallesøe. A non-linear upscaling approach for wind turbine blades based on stresses. In *European Wind Energy Conference and Exhibition, Brussels, Belgium*, pages 1–8. The European Wind Energy Association, 2011.

[35] Jason Mark Jonkman, Sandy Butterfield, Walter Musial, and George Scott. Definition of a 5-mw reference wind turbine for offshore system development, 2009.

[36] SA Ning. Ccblade documentation. `http://www.nrel.gov/docs/fy13osti/58819.pdf`, 2013. Accessed 12-February-2016.

[37] Niels Otto Jensen. *A note on wind generator interaction*. 1983.

[38] Ángel Jiménez, Antonio Crespo, and Emilio Migoya. Application of a les technique to characterize the wake deflection of a wind turbine in yaw. *Wind energy*, 13(6):559–572, 2010.

[39] I Katic, J Højstrup, and Niels Otto Jensen. A simple model for cluster efficiency. In *European Wind Energy Association Conference and Exhibition*, pages 407–410, 1986.

[40] WE Leithead, S De la Salle, and D Reardon. Role and objectives of control for wind turbines. In *IEE Proceedings C (Generation, Transmission and Distribution)*, volume 138, pages 135–148. IET, 1991.

[41] Turaj Ashuri, GJW Van Bussel, MB Zaaijer, and GAM Van Kuik. Controller design automation for aeroservoelastic design optimization of wind turbines. In *The Science of making Torque from Wind, Heraklion, Crete, Greece*, pages 1–7. European Wind Energy Association, 2010.

[42] Fernando D Bianchi, Hernan De Battista, and Ricardo J Mantz. *Wind turbine control systems: principles, modelling and gain scheduling design*. Springer Science & Business Media, 2006.

[43] Turaj Ashuri. *Beyond classical upscaling: Integrated aeroservoelastic design and optimization of large offshore wind turbines*. PhD thesis, Delft University of Technology, the Netherlands, 2012.

[44] AD Platt and M Buhl. Wt perf user guide for version 3.05. Technical report, 00. Tech. rep., National Renewable Energy Laboratory, Golden, CO, 2012.

[45] S Andrew Ning. A simple solution method for the blade element momentum equations with guaranteed convergence. *Wind Energy*, 17(9):1327–1345, 2014.

[46] Jason M Jonkman and Marshall L Buhl Jr. Fast user's guide. *National Renewable Energy Laboratory, Golden, CO, Technical Report No. NREL/EL-500-38230*, 2005.